Eur. Phys. J. Plus (2022) 137:1053
https://doi.org/10.1140/epjp/s13360-022-03276-4

THE EUROPEAN PHYSICAL JOURNAL PLUS

Regular Article

String-based models analysis of proton, $\pi^{\pm}$ and $K^{\pm}$ production in central ^{7}Be +^{9} Be collisions at CERN SPS energies

Khaled Abdel-Waged[a], **Nuha Felemban**

Physics Department, Faculty of Applied Science, Umm Al-Qura university, Makkah 21421, Saudi Arabia

Received: 25 June 2022 / Accepted: 5 September 2022

Abstract We describe how string-based models such as HIJING and PYTHIA8/Angantyr models describe proton, $\pi^{\pm}$ and $K^{\pm}$ rapidity and transverse momentum (p_{T}) spectra from the 20% most central Be+Be collisions at the beam momentum range of 19 AGeV/c to 150 AGeV/c, recently measured in NA61/SHINE experiment at CERN. The HIJING model is extended with a more modern version of PYTHIA (version 6.4), which includes both the hard QCD and standard Lund string routines of PYTHIA8. As for Angantyr, the initial conditions for light nuclei ($A \leq 16$) are updated with a GLISSANDO (Glauber initial state simulation and more) harmonic oscillator shell (HOS) model density profile. It is found that different treatments of diffractive-like events implemented in both models do not lead to a satisfactorily description of the identified hadron spectra. We also compare the PYTHIA8/Angantyr/HOS results using two different mechanisms of the string break-up during the hadronization process, namely, the traditional one (Schwinger-model like) and the thermal one, where each hadron from string breaking is assigned an exponential hadron mass suppression weight times relevant spin and symmetry factors. Good agreement is generally obtained with the thermal model calculations at the whole SPS energies. In particular, it is found that the thermal model is more suited for the description of the identified hadron rapidity and p_{T} spectra, where there are more pions and kaons produced, and fewer protons at midrapidity ($0 < y < 0.2$).

1 Introduction

String-based models such as HIJING [1–3] and PYTHIA8/Angantyr [4, 5] have been constructed for the description of heavy-ion collisions (HIC) at Large Hadron Collider (LHC) energies. While the global tuning of the models is in good agreement with the data at LHC [2, 3, 5–7], there are significant discrepancies in describing data at lower center of mass energies [8, 9]. These disagreement may be due to the fact that the primarily highly energetic nucleon-nucleon (NN) (sub)collisions during the first stage of HIC rely on perturbative cross sections and can only be applied at large momentum transfers, while the secondary interacting nucleons (where one of projectile/target nucleons has already been interacted) suffer a longitudinal momentum exchange with a distribution $\propto dQ/Q$, leading to longitudinal string excitations and subsequent hadronization phase that cannot be treated as a perturbative process. Thus, one has to rely on nonperturbative models to describe the soft processes in HIC.

Both HIJING [1–3] and PYTHIA8/Angantyr [5] use different approaches for the generation of diffractive-like events during the interaction processes, while the subsequent evolution and hadronization of these excited events are based solely on the Lund string fragmentation scheme [10]. In Angantyr [5], a given nucleon of the projectile nucleus (N_i, $i = 1, 2, 3, ...A$) interacts inelastic nondiffractively with several nucleons from the target nucleus (N_j, $j = 1, 2, 3, ...B$). Only one primarily NN_j collision is handled as hard NN (sub)collision, with a slightly reduced energy, while the others NN_{j-1}, are treated as single diffractive (SD) excitation events, with significantly reduced energies. The single diffractive (SD) excitation events are modeled as nondiffractive interactions between the target nucleons and a Pomeron emitted from a projectile nucleon. Pomeron fluxes define the mass of diffractive systems, resulted in low mass and high-mass diffractive events [11]. HIJING [1], instead, relies on Glauber calculations to determine the number of inelastic NN-(sub)collisions, which are of two types: soft NN-processes treated as in FRITIOF [12–14] and hard parton-parton collisions treated as in PYTHIA. The soft interacting nucleons in HIJING lead to an excited mass $\propto dM^2/M^2$ similar to a contribution from an SD excited event in the Angantyr model [5].

In the Lund string model [10] quark-antiquarks ($q\bar{q}$) or diquark-antidiquark ($qq\bar{q}\bar{q}$) pairs are produced as strings break when the partons move away from each other, described by a tunneling process using Schwinger model-like [15]. Until the strings reduce to small pieces, this process continues. Hadrons are formed from these string pieces by assigning a Gaussian distribution in transverse

[a] e-mail: kamabdellatif@uqu.edu.sa (corresponding author)

Published online: 15 September 2022

momentum ($p_\perp$) to quarks, and, by addition, to hadrons [10], while its longitudinal momentum is determined by the Lund symmetric fragmentation function [16].

The Lund model [10], realized within the PYTHIA models [4, 17], is successful in describing a huge variety of observables at high energies [7, 18]. The PYTHIA event generator [17] is incorporated in many microscopic transport calculations such as UrQMD [19], GiBUU [20], PHSD [21] and SMASH [22] to describe the hadronization of an initial parton configuration in HIC at high energies. However, cracks started to appear in the picture as new CERN SPS data have been presented [23, 24]. Specifically, a recent comparison of the measured rapidity and transverse momentum distributions at NA61/SHINE data to UrQMD (version 3.04) shows large discrepancies between the model and data at different SPS energies [23]. It was also shown in Ref. [25] that the PHSD model (which includes partonic interactions in-and-out of equilibrium, Lund generator of PYTHIA 6.4 [17] and final interactions of hadrons) was not able to describe the rapidity distributions of π^- in inelastic pp-collisions at $\sqrt{s_{\rm NN}} = 6.2$, 7.6, 8.8 and 12.3 GeV. The same holds for the description of proton and π^- $p_{\rm T}$-spectra at midrapidity ($0 < y < 0.2$) [25].

In the present work, the HIJING (version 1.383) code [1] is extended with a more modern version of PYTHIA (version 6.4) [17], which includes both the hard QCD and the standard Lund string routines of PYTHIA8 [4]. As for Angantyr [5], the initial conditions for light nuclei ($A \leq 16$) are updated with a GLISSANDO (Glauber initial state simulation and more) harmonic oscillator shell (HOS) model density profile [26]. We systematically apply the improved HIJING (ImHIJING) [27] and PYTHIA8/Angantyr/HOS models to the 20% most central ^{7}Be+^{9}Be collisions at CERN SPS energies and investigate the differences between the models by comparing the results obtained by these string-based models with the recent NA61/SHINE data of proton, $\pi^\pm$ and $K^\pm$ rapidity and transverse momentum spectra [24]. The detailed study of ^{7}Be+ ^{9}Be collisions is important not only because they represent the lowest mass isospin symmetric reference system but also the yield ratio of strange hadrons to pion is found close to those in central Pb+Pb collisions and significantly higher than in proton-proton (pp) interactions [28, 29].

We also provide a detailed comparison of PYTHIA8/Angantyr/HOS results using two different tunneling mechanisms of the string break-up during the hadronization process, namely, the traditional Schwinger-like [10] and thermal [30] $p_\perp$ suppressions. The Schwinger model [10] is used, as in the standard Lund model, to calculate the transverse momentum ($p_\perp$) of the hadron, where it receives its $p_\perp$ as the vector sum of its Gaussian quark(antiquark) constituent kicks, whereas the thermal model [30], inspired by thermodynamics, calculates the transverse mass $m_{\perp \rm had}$ of all hadrons whose flavor content includes the incoming quarks when an old q flavor is always known. The thermal model is intended to enhance low $p_\perp$ lighter-meson production and deplete baryon one. In contrast, all hadrons receive the same $p_\perp$ spectrum for the traditional Schwinger model.

We note that earlier analyses have been performed in Ref. [31], where one of the authors have used the thermal model approach to study the precedent NA61/SHINE data set including only spectra of negatively charged pions produced in central ^{7}Be+ ^{9}Be and ^{40}Ar +^{45} Sc collisions at CERN SPS energies [32, 33]. With the existence of new data from the NA61/SHINE collaboration [24] which cover now the inclusive spectra of proton, $\pi^\pm$ and $K^\pm$ produced in 20% central ^{7}Be+ ^{9}Be collisions at all available SPS energies, we consider it is necessary and important to present in this paper the first comparisons of both the rapidity and transverse momentum spectra of these most recent data to the thermal model calculations. As shown below, implementation of both the proper diffractive-like events and tunneling mechanisms in PYTHIA8.303/Angantyr/HOS is essential as it sets the foundation for the prediction of proton stopping in central light ion beams at CERN SPS energies [24].

The manuscript is organized as follows: In Sect. 2, we define the basic ingredients of the HIJING and PYTHIA/Angantyr models. In Sect. 3 we confront the updated models to measurements from NA61/SHINE [24] experiment. Finally, in Sect. 4 we present our conclusions.

2 Description of the models

2.1 PYTHIA8/Angantyr model

PYTHIA8 [4] is a Monte Carlo event generator used to simulate proton-proton collisions at Large Hadron Collider (LHC) energies. For this study we have used PYTHIA version 8.303 to simulate nucleus-nucleus (AA) collisions with Angantyr [5]. Angantyr model combines several nucleon-nucleon (NN) collisions into one heavy-ion collisions. The model includes three main ingredients: (i) an advanced Glauber model, including Gribov corrections of diffraction excitation and color fluctuations to generate the number of sub-collisions [34]; (ii) the full power of PYTHIA8 pp machinery to describe individual nucleon-nucleon (NN) (sub)collisions [4]; and (iii) a framework for close packing of strings, which explores systematic effects on the string tension in a denser string environment [30].

In Angantyr, positions and the number of wounded (participating) nucleons are determined by standard Glauber model-based eikonal approximation in impact-parameter space [35]. The positions of nucleons in the two nuclei are generated according to a two-dimensional Saxon-Woods (SW) distribution in the GLISSANDO (Glauber initial state simulation and more) parameterization [26], applicable for heavy-nuclei with $A > 16$.

Each nucleon in the projectile nucleus may interact with several nucleons in the target nucleus and vice versa. The interacting pairs of projectile/target nucleons are ordered in a list in an increasing NN-impact parameter. The advanced Glauber model, inspired by color fluctuations, has been employed in order to generate a corresponding sub-event between a nucleon in the projectile and

nucleon in the target, and the corresponding nucleons are characterized as diffractively or absorptively (nondiffractive) wounded. The fluctuations in the nucleons were fitted to the default parameterizations of semi-inclusive cross sections in PYTHIA8 [4]. If an interaction is found in the list where one of the nucleons has already interacted, this will be marked as secondary and the generated sub-event will be added to the sub-event to which the already interacted nucleons belong. This gives a set of primary absorptive collisions and a set of secondary ones. The primary absorptive collisions are classified as hard subcollisions and treated using the full power of multiparton interaction (MPI) machinery of PYTHIA8 [4]. On the other hand, the secondary absorptive sub-collisions are generated as a dynamical Regge-based model for interactions between one projectile and several target nucleons. The contribution from a secondary absorbed nucleon is similar to the contribution from an excited nucleon in a single diffraction event. These are treated using the single diffractive (SD) machinery of PYTHIA8 [5].

The soft part of PYTHIA8/Angantyr is based on FRITIOF and Lund string fragmentation schemes [10, 12–14]. The former determines the invariant masses of the excited string, which are formed due to inelastic NN-scattering between valence quarks or diquarks, while the latter treats the decay of the strings into new ones by quark-antiquark ($q-\bar{q}$) or diquark-antidiquark ($qq-\bar{q}\bar{q}$) pair production.

In the Lund scheme [10], the species of the fragmented hadron follows from the flavor of the $q-\bar{q}$ or $qq-\bar{q}\bar{q}$ pair that is produced. As the quark q and antiquark ($\bar{q}$) move apart, the string may break by the production of a new "vertex" pair $q'-\bar{q}'$. The rate of $q'-\bar{q}'$ string break is assumed to be given by Schwinger formula [15]

$$P \propto \exp(-\pi m_{\perp q'}^2/k), \tag{1}$$

where $2m_{\perp q'} = 2\sqrt{m_{q'}^2 + p_{q'\perp}^2}$ is the transverse mass of the pair of quarks with mass $m_{q'}$ and transverse momentum $p_{q'\perp}$. The q' and $\bar{q}'$ receive $p_{q'\perp}$ characterized by a Gaussian width $\sigma_{q'q'}$. The transverse momentum of a hadron ($p_{T\mathrm{had}}$) is given by a vector sum of its q' and $\bar{q}'$ kicks, and thus $\langle p_{T\mathrm{had}}^2 \rangle = 2\sigma_{q'q'}^2$. While the light quarks have the same probability to be produced, there are empirical suppressions for producing heavier quarks and diquarks [15]:

$$\gamma_{Q'\bar{Q}'} = \frac{P_{Q'-\bar{Q}'}}{P_{q'-\bar{q}'}} = \exp\Big(-\pi\Big(m_{\perp Q'}^2 - m_{\perp q'}^2\Big)/k\Big). \tag{2}$$

For the vacuum string tension value $k = 1$ GeV fm^{-1}, the above equation results in a suppression of heavier quark production according to $u : d : qq : s \simeq 1 : 1 : 0.02 : 0.3$ [10].

PYTHIA8 also implements the simple popcorn mechanism for better account of baryon production, based on the Lund string fragmentation scheme [10]. It is assumed that new baryons (B) and antibaryons ($\bar{B}$) are formed as neighbors or next to neighbors in a string break-up when vertex $q'q'-\bar{q}'\bar{q}'$ pairs are recombined with surroundings quarks and antiquarks. The density and size of the color fluctuations will determine the properties of the $B\bar{B}$ production channel. It is also possible to create another quark and antiquark pair in the color field spanned by the $q'q'-\bar{q}'\bar{q}'$ pair. This leads to the production of one or a few mesons between the $B\bar{B}$ pairs along the string, i.e., the $BM\bar{B}$ configuration channel. It should be noted here that the popcorn model implemented in PYTHIA8 allows for maximum one meson to be produced in-between, even though the general model in principle could allow for more.

The simple popcorn mechanism of the Lund model contains a number of parameters to describe the outcome of the string/tunneling mechanisms for particle production. In the implementation we adopt the Monash 2013 tunes that govern quark-level suppression of the light meson and baryon production [6]. It should be stressed that the particle masses do not enter explicitly in the Lund string fragmentation scheme.

In the current version of Angantyr included in PYTHIA8, the thermal model option has been included to string fragmentation. Unlike statistical models, it is based on the Lund string fragmentation scheme, but in which the production rates are determined by the hadron masses rather than by the quark properties [36–39]. In the thermal model, the suppression factor for producing hadron of transverse mass $m_{\perp\mathrm{had}}$ in a string with energy density T is estimated by [30]

$$P_{had}(m_{\perp had}) = \exp(-m_{\perp had}/T), \tag{3}$$

with $m_{\perp\mathrm{had}} = \sqrt{m_{\mathrm{had}}^2 + p_{\perp\mathrm{had}}^2}$ and $T \sim \sqrt{k/\pi} = \sigma$ is the string energy per unit length. Such $m_{\perp\mathrm{had}}$ shape has some foundation in the Hagedorn temperature [36] and related ideas [37–39]. In more detail, each $q'-\bar{q}'$ break-up is associated with a modified Bessel $p_{\perp q'}$ distribution such that the two-dimensional convolution results in an $\exp(-p_{\perp\mathrm{had}}/T)$ spectrum [30]. In each fragmentation step, an old q flavor is known when the new one is selected and a hadron is produced out of the two. Each new quark and hadron is assigned a relative weight given by Eq. (3).

Depending on the hadron species, the probability in Eq. (3) receives additional multiplicative factors: (i) vector mesons receive a factor of 3 and tensor mesons a factor of 5, (ii) diagonal meson mixing factors are included, (iii) a free overall normalization factor is received for baryons with respect to mesons, (iv) octet baryons with three different flavors receive different internal spin configurations, and finally (v) an extra suppression factor for hadrons with strange (di)quarks is included (γ_s'). Note that points (ii) and (iii) have also been included in the standard Lund model. All probabilities are then rescaled to sum up to unity, and the hadron

species is chosen accordingly. The thermal model does not include simple popcorn baryon production mechanism, i.e., no mesons are produced between B and $\bar{B}$.

The momentum of the hadron is constrained by the already determined hadron transverse mass $m_{\perp \mathrm{had}}$, $E^2 - p_z^2 = m_{\perp \mathrm{had}}^2$. The longitudinal momentum (p_z) carried by a hadron is determined for both the thermal and standard Lund models using the symmetric fragmentation function [16]

$$f(z) \propto \frac{1}{z}(1-z)^a \exp\left(-\frac{bm_{\perp \mathrm{had}}^2}{z}\right), \tag{4}$$

where a and b are the free parameters of the model. Here z is the fraction of $E + p_z$ taken by the produced hadron, out of the available $E + p_z$. The remaining (light-cone) energy fraction $(1 - z)$ goes to the new string system, from which another hadron can be split off until all the energy is used up.

At the earliest times before hadronization, PYTHIA8 also includes the possibility of increasing string tension in a denser string environment [30]. This is a consequence of the PYTHIA model for MPIs which lead to a closer packing of strings (CPS) in the event, but preserve their separate identities. In this model [30], the creation of a hadron is begun by an exploratory step ahead, so that the number of strings overlapping the rapidity range of the next hadron can be estimated. The momentum of the average expected hadron is defined by using an average hadron mass and $p_\perp$, defined in the frame of the parent string. The number of strings (n_{string}) that crosses the rapidity of the expected hadron is then determined. For low $p_\perp$ hadroproduction, the rapidity of the endpoint partons of each string pieces is given by [30]

$$y = \mathrm{sgn}(p_z) \log \frac{E + |p_z|}{\sqrt{max(m_\perp^2, m_{min}^2)}}, \tag{5}$$

where m_{min}^2 has the purpose to protect against strings with low $m_\perp$ endpoints from populating the full rapidity range. The effective number of strings is calculated as [30]

$$n_{\mathrm{string}}^{\mathrm{eff}} = 1 + \frac{n_{\mathrm{string}} - 1}{1 + p_{\perp \mathrm{had}}^2 / p_{\perp 0}^2}, \tag{6}$$

where $p_{\perp \mathrm{had}}$ is transverse momentum of the created hadron and $p_{\perp 0}$ is the MPI regularization parameter. Using Eq. (8), the temperature in Eq. (5) is modified due to close packing of strings as [30]

$$T \rightarrow \left(n_{\mathrm{string}}^{\mathrm{eff}}\right)^r T, \tag{7}$$

where r is a free parameter of the model that gives a rescaling factor for the CPS.

2.2 HIJING model

HIJING [1] is built with similar starting point as Angantyr. It relies on Glauber calculations to determine the number of NN-(sub)collisions. Particles produced from two colliding nucleons at high energy ($\sqrt{s_{\mathrm{NN}}} > 4$) GeV are described by hard and soft components. The hard component involves processes in which multiple hard partonic subcollisions are generated with transverse momentum p_{T} larger than a transverse momentum cut off p_0. The inclusive cross section of the multiparton interactions (MPI) is described by perturbative QCD, which depends on the parton distribution function (PDF) and $p_{\perp \mathrm{min}}$ scale of the regularization factor, given by Eq. 8. The kinematics of the jets and the associated initial and final state radiations are simulated by PYTHIA model [17]. On the other hand, the soft component ($p_{\mathrm{T}} < p_0$), characterized by a soft cross section σ_{soft}, treats nonperturbative processes and is modeled using the assumptions of FRITIOF and Lund string fragmentation scheme, through JETSET/PYTHIA routines [10].

The main differences between Angantyr and HIJING at intermediate energies ($\sqrt{s_{\mathrm{NN}}} \leq 20$ GeV) are the treatment of the fluctuations and the generation of diffractive-like events. While Angantyr accounts for fluctuations in the initial states of individual nucleons, and in the positions of nucleons within the two nuclei, HIJING does neither. Angantyr models diffractive excitation as nondiffractive interactions between the target nucleons and a Pomeron emitted from the projectile. Pomeron flux defines the mass spectrum of diffractive systems, resulted in low-mass or high-mass diffraction events. For low-mass diffraction, ≤ 10 GeV, the excited system is modeled as simple string treated using Lund string fragmentation scheme. As for high-mass diffraction, PYTHIA8 treats a Pomeron-proton collision as nondiffractive hadron-hadron collision and uses the full MPI machinery. In contrast, HIJING treats soft processes using a scheme for soft interactions similar to FRITIOF model with some differences in the successive soft excitations of the leading quarks/diquarks and p_{T} transfer involved. The multiple soft gluon exchange between valence quarks/diquarks of the two colliding hadrons leads to longitudinal string like excitations. Gluon production from hard processes and soft radiations is included as kinks in the strings. In the end all partons in HIJING are connected by strings and hadronized by the Lund string fragmentation scheme [10].

In order to demonstrate the differences between the models used, we present in Fig. 1 the proton rapidity distributions in the 20% most central ^{7}Be+ ^{9}Be collisions: The PYTHIA8/Angantyr results with/without diffractive events are compared with the corresponding HIJING calculations. Clearly we get a somewhat similar shape for both calculations when diffractive excitation is

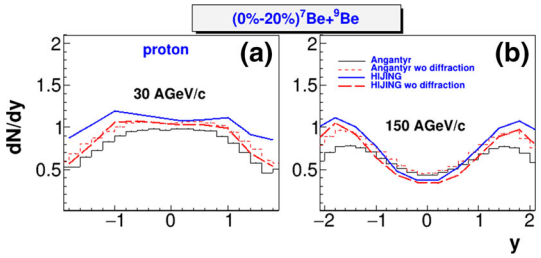

Fig. 1 (COLOR ONLINE) Rapidity distributions of protons in the 20% most central ^{7}Be+ ^{9}Be collisions for zero diffractive excitation in PYTHIA8/Angantyr and HIJING models. For comparisons the results from diffractive events of both models are also shown

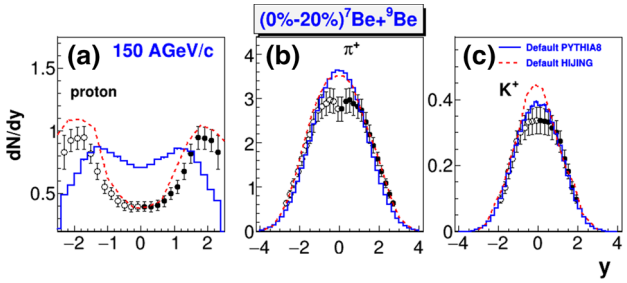

Fig. 2 (COLOR ONLINE) Rapidity distributions of protons, π^+ and K^+ in the 20% most central ^{7}Be+ ^{9}Be collisions at 150 AGeV/c in the default PYTHIA8/Angantyr and HIJING models

zero, especially at low SPS energies. We notice that including diffractive (fluctuations) events in PYTHIA8/Angantyr resulted in a reduced proton dN/dy in central light-ion collisions. On the other hand, diffractive events in HIJING lead to enhancement of proton dN/dy covering all rapidity range. Thus, in contrast to HIJING, the diffractive excitation in Angantyr acts as part of shadow scattering caused by primary inelastic (nondiffractive) channels. This indicates that the different treatments of diffractive excitation implemented in the studied string-based models will have a quite significant effect for the final particle multiplicity, as discussed below in sect. 2.

In this work, the identified particle yields in light-ion collisions are investigated by employing an updated version of HIJING (ImHIJING) [27] incorporated with a modern version of PYTHIA (version 6.4). Note that, the two programs JETSET and PYTHIA 5.2 are merged under the PYTHIA6.4. Most of the physics aspects in PYTHIA8, including both soft and hard QCD routines, are unchanged relative to PYTHIA6.4.

2.3 Numerical results

To see the influence of various physical ingredients of string-based models on the particle production of protons, charged pions and charged kaons in 20% central Be+Be collisions, three types of calculations were performed: (i) Angantyr calculations with standard Lund fragmentation scheme, (ii) Angantyr calculations with thermal model, and (iii) the same as (i) but with ImHIJING calculations.

Physics processes implemented in HIJING and PHYTHIA8/Angantyr generators include multiple parameters which are tuned to experimental measurements from proton-proton collisions at RHIC and LHC energies. At higher SPS energies, both models are incompatible with NA61/SHINE data, see Fig. 2. In particular, both models overestimate the newly produced hadrons at midrapidity independent of the degree of stopping of Be nuclei. These disagreements can mainly be understood as a consequence of incorrect tunning of multi-partonic interactions (MPI) and string formation/fragmentation mechanisms. The multiparton interactions (MPI) setting parameters of PYTHIA6.4 have been chosen to match with pp-tune PYTHIA8 at SPS energies [40]. Because the stopping of baryons in light-ion collisions is mostly determined by the first interactions of the participants, all of the models under study are tuned to fit the rapidity and transverse momentum spectra of $\pi^{\pm}$, $K^{\pm}$ and protons in inelastic pp-collisions at CERN SPS energies [27, 40]. Table 1 presents the most important parameters that affect soft particle production. The PYTHIA8/Angantyr calculations are simulated using Monash 2013 tunes that govern quark-level suppression of the light meson and baryon production [6]. Note

Table 1 Parameter sets of Angantyr and ImHIJING models for Be+Be collisions

	a	b GeV^{-2}	$\gamma_{q'q'}$	γ_s	$\sigma_{q'q'}$ GeV/c
PYTHIA8/Angantyr	0.68	0.98	0.081	0.217	0.335
ImHIJING	0.5	0.9	r 0.07	0.22 γ_s'	0.35 T GeV/c
Thermal model			0 – 0.5	0.4	0.31

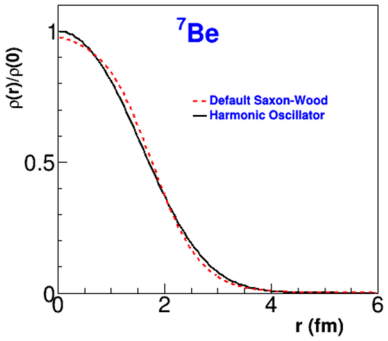

Fig. 3 (COLOR ONLINE) Nuclear density distributions for ^{7}Be nucleus. The thin-dashed line represents the default Saxon-Woods density profile implemented in PYTHIA8/Angantyr, while the solid line is the GLISSANDO harmonic oscillator density distribution

that both the default MPI and Lund string fragmentation parameters of ImHIJING are tuned in view of a closer comparison with Angantyr.

3 Results and discussion

In this section we systematically apply PYTHIA8/Angantyr (version 8.303) and ImHIJING codes to 20% central ^{7}Be+^{9}Be collisions at incident projectile momentum of 19, 30, 40, 75, and 150 AGeV/c (which corresponds to $\sqrt{s_{\rm NN}} = 6.1$, 7.6, 8.8, 11.9, and 16.8 GeV, respectively) and investigate the differences between these models by comparing them with the recent NA61/SHINE measurements of the rapidity distributions (dN/dy) and transverse momentum ($p_{\rm T}$) spectra of protons, charged pions and kaons [24]. Because dN/dy are measured in minimum bias, we generate 10^5 events for the $0\% - 20\%$ centrality bin. We use for the 20% centrality class the forward energy (EF) selection of the GLISSANDO model provided in Table 1 of Ref. [24], which corresponds to the smallest number of the projectile (^{7}Be) spectator nucleons. The analysis range of $p_{\rm T}$ spectra is restricted to the measured midrapidity range of $0 < y < 0.2$.

As already mentioned in Sect. 2, four separate components are needed for Angantyr/ImHIJING generalization of pp-collisions to an event generator for AA-collisions: (i) It is necessary to generate nucleon distributions inside the nucleus, (ii) one has to calculate the number of interacting nucleons, where the projectile nucleons are assumed to undergo multiple NN-(sub)collisions with nucleons in the target, (iii) one must estimate the contribution to soft particles from NN-collisions, calculated using the Lund string fragmentation scheme, and (iv) it is necessary to account for hard partonic NN (sub)collisions, generated using the full MPI machinery of PYTHIA.

Monte Carlo event generator such as PYTHIA6.4/PYTHIA8 [4, 17] has parameters which has to be adjusted to control the behavior of the event modeling in proton-proton collisions. As discussed in Ref. [40], the $p^2_{\perp\rm min}$ scale of the regularization factor $p^4_T/(p^2_{\perp\rm min} + p^2_T)^2$ is important to account for the dampening of the MPI cross section ($\sigma_{\rm int}$) at $p_{\rm T} \to 0$. In the default PYTHIA6.4/PYTHIA8, $p^2_{\perp\rm min}$ is given by [4, 17]

$$p^2_{\perp\,\rm min}(s) \;=\; p^2_{\perp 0}\left(\frac{s}{s_{ref}}\right)^{\varepsilon}, \tag{8}$$

with $p_{\perp 0} = 2.28$ GeV/c and some power ϵ that sets the scaling away from $s = s_{\rm ref} = E^2_{CM}$. The default value for the scaling power in PYTHIA6.4(PYTHIA8) was $\epsilon = 0.215$ for the $E_{CM} = 1800(7000)$ GeV reference energy [6, 17]. The settings that are varied in our tune are the reference energy, $s_{\rm ref}$, and the energy dependence scaling (ϵ) [40]. We have changed the reference energy to be $E_{CM} = 10$ GeV and the power of energy rescaling to $\epsilon = 0.16$ to control the power law extrapolation as much as possible at low center of mass energies. The value $\epsilon = 0.16$ is motivated by relating it to the scaling of the energy dependence of the total pp cross section ($\sigma_{\rm tot}$) via Regge phenomenology [41], which grows like $\propto E^{0.16}_{\rm cm}$.

As shown in Ref. [40], even going below the reference energy of $E_{CM} = 10$ GeV, PYTHIA8 with tuned MPI settings gives a very reasonable description of the measured proton, $\pi^{\pm}$ and $K^{\pm}$ spectra in inelastic pp-collisions at the whole SPS energies. In the following we systematically apply the tuned MPI settings in both ImHIJING and PYTHIA8/Angantyr to explore the transition of the reaction dynamics from proton-induced reactions to light-ion collisions at the SPS energies.

To correctly model nucleus-nucleus (AA) collision processes in the Angantyr framework, one needs the distributions of centers of nucleons in the considered nuclei. In the public version of PYTHIA8/Angantyr model, nucleon positions of light nuclei with mass number $3 \le A \le 16$ are not implemented. In this work, we have used a GLISSANDO harmonic oscillator shell (HOS) model distribution [26] in the PYTHIA8/Angantyr model to study Be+Be collisions, and with a nuclear repulsion effect implemented as a

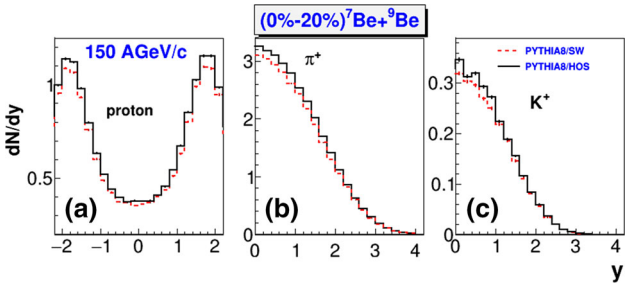

Fig. 4 (COLOR ONLINE) Rapidity distributions of proton, π^+ and K^+ in central Be+Be collisions at 150 AGeV/c. The short-dashed and solid lines denote PYTHIA8/Angantyr calculations using GLISSANDO Saxon-Woods and harmonic oscillator density profiles, respectively

hard-core radius of $d = 0.9$ fm for each nucleon, below which two nucleons cannot overlap. The HOS nucleon density distribution is parameterized as [26]

$$\rho(r) = \frac{4}{\pi^{3/2}C^3}\left[1 + \frac{A-4}{6}\left(\frac{r}{C}\right)^2\right]e^{-r^2/C^2},$$
$$C^2 = \left(\frac{5}{2} - \frac{4}{A}\right)^{-1}\left(< r_{ch}^2 >_A - < r_{ch}^2 >_p\right) \tag{9}$$

where $< r_{ch}^2 >_A$ and $< r_{ch}^2 >_p$=0.7714 fm^2 are the mean squared charge radii of the nucleus and proton [26]. The values of the harmonic shell model parameter $< r_{ch}^2 >_A$= 6.69 and 6.0 fm^2 for ^{7}Be and ^{9}Be, respectively [26]. Figure 3 shows the calculations for HOS ^{7}Be nucleus compared to the default Saxon-Woods case. We note from Fig. 3 that the HOS increases ^{7}Be nucleon density at the center compared to the default Saxon-Woods case. Our basic findings, presented in Fig. 4, are that HOS structure in light nuclei leads to an increase of the proton, π^+ and K^+ yields in collisions with 20% central ^{7}Be+^{9}Be collisions. The effect is most manifest for the produced hadrons at central rapidity ($0 < y < 1$), where high multiplicity collisions occur. In what follows, all PYTHIA8/Angantyr calculations are performed using HOS density profile.

We start with a comparison of Angantyr results (short-dashed lines) with ImHIJING results (thin lines) and NA61/SHINE data on proton rapidity spectra in 20% central Be+Be collisions at different SPS energies as presented in Figs. 5, 6, 7, 8, 9, 10, and 11. Both models use the same Lund string fragmentation scheme and are adjusted in order to get a better agreement with experimental data for inelastic pp collisions at CERN SPS energies [27, 40]. As discussed above, the main source of difference between the two models is the generation of diffractive-like events, which are formed due to NN-(sub)collisions. We note that in the current version of Angantyr both the (non)diffractively excited and secondary absorbed nucleons produce a string with mass distributed as dM^2/M^2. In HIJING, however, excited nucleons are mainly produced from soft NN-collisions which generally involve single(double) diffractive interactions.

Figure 5 shows that ImHIJING tends to have more stopping at low beam energies ($\leq$ 40 GeV/c) and more transparency at high beam energies. One can see that the p dN/dy agrees better with ImHIJING at the top SPS energy, while the midrapidity region is reproduced by both models. At the lowest SPS energy the ImHIJING calculations show a somewhat triangular shape. This behavior is due to the fact that the single diffractive (SD) events in HIJING are produced from a simple flat string, as implemented in FRITIOF, with mass distributed as dM^2/M^2, when hadronizing to a color string gives the triangular shape behavior in rapidity. In contrast, we notice in Fig. 5 that using PYTHIA8/Angantyr SD machinery for both soft NN-diffractively excited and secondary absorbed nucleons result in too little activity as the collision energy decreases. At intermediate SPS energies (30 and 40 AGeV/c) both models overshoot the measured data and give too flat distributions, which is attributed to larger values of M.

In Fig. 6 we show Angantyr and ImHIJING comparisons to NA61/SHINE data for proton p_T spectra at midrapidity ($0 < y < 0.2$). We find that different treatments of diffractive-like events have a quite significant effect on the proton spectra at midrapidity for the whole SPS energies. Comparing ImHIJING to Angantyr, we see that ImHIJING increases the proton low-p_T spectra as the collision energy decreases. This implies that the interacting nucleons in ImHIJING produce an overall larger amount of excited diffractive events, which is inconsistent with the measurements at lower SPS energies. We also notice that Angantyr well describes the whole proton p_T spectra at the lowest SPS energy better than ImHIJING. As for higher SPS energies, the Angantyr model is clearly not perfect at low p_T, but nevertheless gives a fair description at $p_T > 0.5$ GeV/c due to the more careful treatment of (non)diffractively excited and secondary absorptive sub-events.

The conclusion from Figs. 5 and 6 is that the PYTHIA8/Angantyr and ImHIJING calculations using different treatments of diffractive-like events can obviously not describe data for the proton rapidity and p_T spectra at CERN SPS energies completely.

We continue with the comparison of the ImHIJING and PYTHIA8/Angantyr results to the experimental data from NA61/SHINE on the rapidity distributions of produced particles in central Be+Be collisions at different SPS energies, which are shown in Figs. 7, 8, and 9. Compared to the data, ImHIJING describes the meson production very well at high energies ($\geq$ 40 AGeV/c), while Angantyr gives better description at lower SPS energies. It should be noted that the calculated rapidity spectra of $\pi^\pm$ and $K^\pm$ in pp-collisions show a similar trend with data as in central light-ion collisions [27, 40]. In particular the ImHIJING results from p+p inelastic collisions are shown to reproduce $\pi^\pm$ and $K^\pm$ rapidity spectra at 40, 80, and 158 GeV/c Ref. [27], while PYTHIA8 calculations

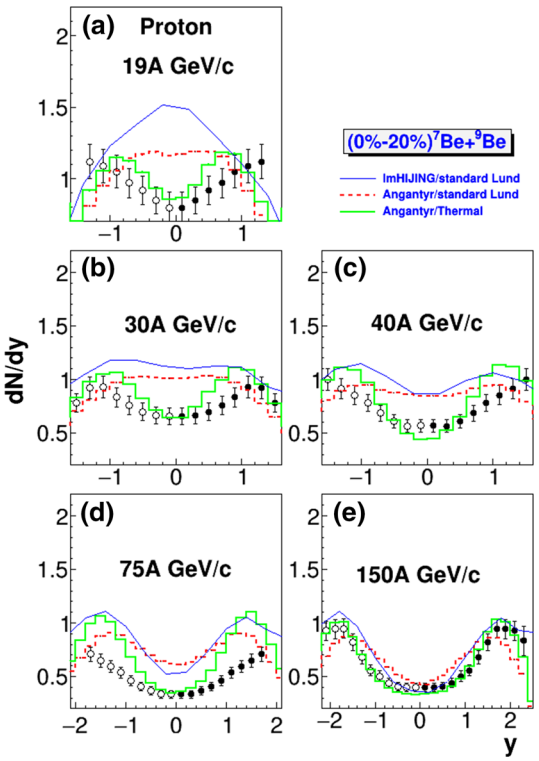

Fig. 5 (COLOR ONLINE) Rapidity distributions of protons in the 20% most central ^{7}Be+ ^{9}Be collisions at different SPS energies. The improved HIJING (ImHIJING) results are plotted by thin lines. Predictions of the PYTHIA8/Angantyr/HOS calculations using standard Lund and thermal models are shown in short-dashed and thick lines, respectively. The data have been symmetrized. The closed points represent NA61/SHINE [24] data, and open points are symmetrized

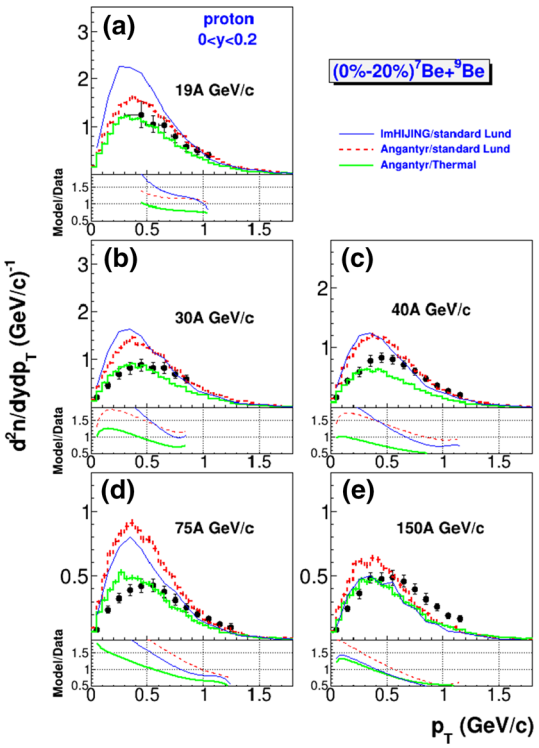

Fig. 6 (COLOR ONLINE) Same as Fig. 3, but for the transverse momentum spectra at midrapidity ($0 < y < 0.2$)

underestimate the charged pion yield at central ($0 < y < 0.7$) rapidity [40]. This is expected because the mechanisms of producing hadrons in light-ion collisions are simulated in a dynamical way similar to elementary hh-collisions.

Figures 10 and 11 show the comparison of ImHIJING and PYTHIA8/Angantyr results for the p_{T} distributions of π^{+} and K^{+} in central light ion collisions at 40, 75, and 150 AGeV/c. At such energies the two models differ only in the degree of proton stopping, where the least stopping is observed with ImHIJING (see Figs. 5(6)c- 5(6)e). One can see that both models agree with the measured data on meson spectra within experimental uncertainties. The agreement between ImHIJING and PYTHIA8/Angantyr is quite good

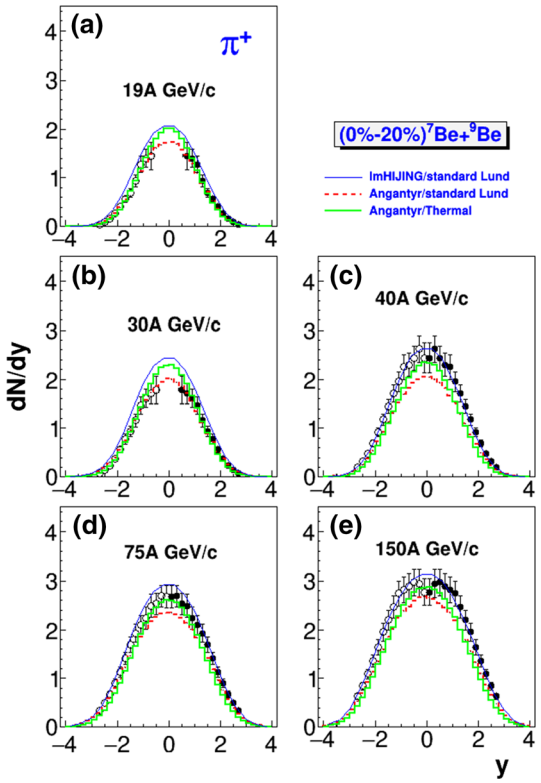

Fig. 7 (COLOR ONLINE) Rapidity distributions of positive pions in the 20% most central ^{7}Be+ ^{9}Be collisions. The ImHIJING results are plotted by thin lines. Predictions of the PYTHIA8/Angantyr/HOS calculations using standard Lund and thermal models are shown in short-dashed and thick lines, respectively.The data have been symmetrized. The closed points represent NA61/SHINE [24] data, and open points are symmetrized

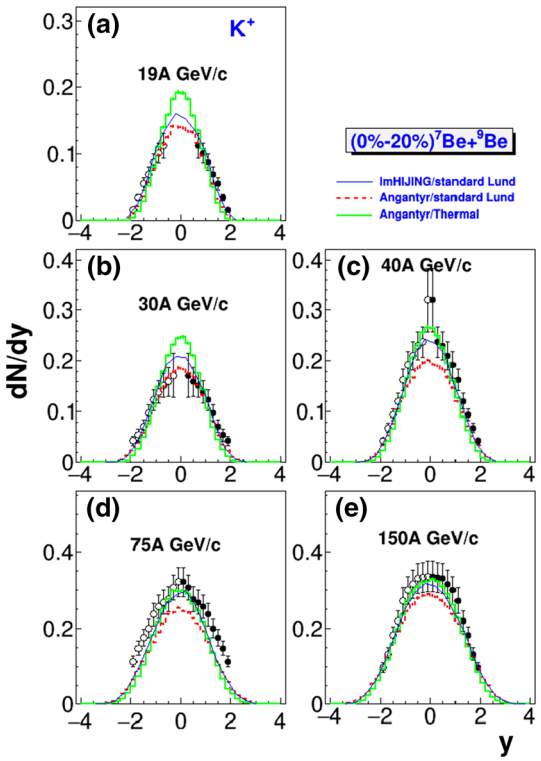

Fig. 8 (COLOR ONLINE) Same as Fig. 7 but for K^{+}

except for the low p_{T} region (< 0.5 GeV/c) where the ImHIJING spectra are higher than PYTHIA8/Angantyr. This indicates that proton stopping not only affects the dynamics of the string before fragmentation, but also the mass of the string, and therefore the energy available for producing new particles.

From this investigation of different event generators employing the same Lund string fragmentation scheme, it is clear that different treatments of generating diffractive-like events do not lead to an overall agreement with NA61/SHINE measurements.

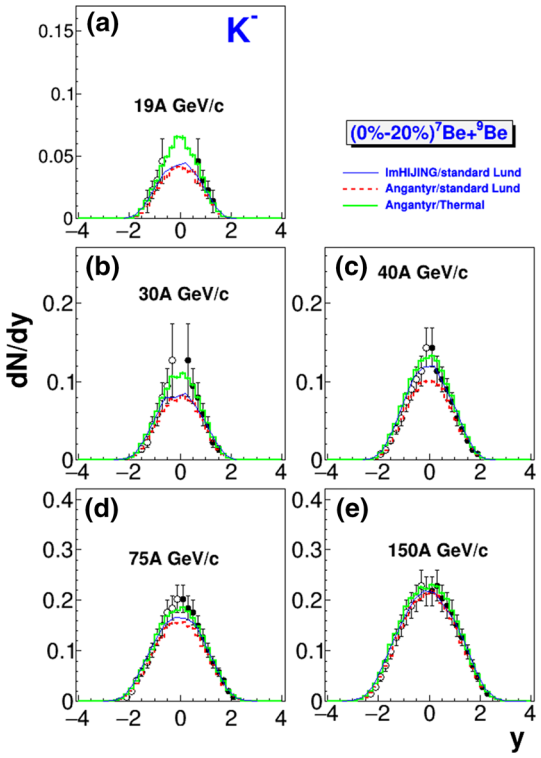

Fig. 9 (COLOR ONLINE) Same as Fig. 7 but for K^-

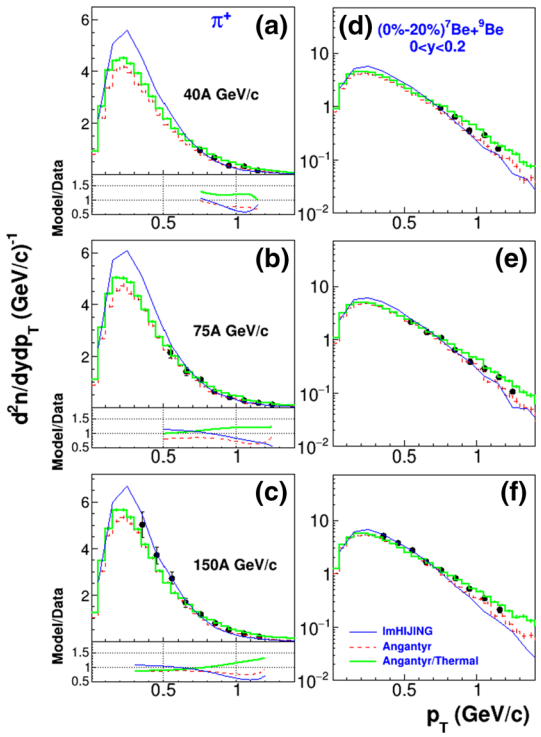

Fig. 10 (COLOR ONLINE) Transverse momentum spectra of positive pions in midrapidity ($0 < y < 0.2$) in the 20% most central ^{7}Be+ ^{9}Be collisions. The ImHIJING results are plotted by thin lines. Predictions of the PYTHIA8/Angantyr/HOS calculations using standard Lund and thermal models are shown in short-dashed and thick lines, respectively. The closed points represent NA61/SHINE data [24]. For the efficient comparisons of the calculations and the data for the whole p_T spectra, we plot the results in linear-linear and semi-log forms

Since proton stopping in light-ion collisions is a physical effect that must be taken into account, this clearly needs further string-model improvements.

Next, we provide a comparison of PYTHIA8/Angantyr results using two different mechanisms of the string break-up during the hadronization process: the traditional one (Schwinger-model-like) and the thermal one. In the standard Lund model, the rate of $q-\bar{q}$ ($qq-q\bar{q}q$) pairs is traditionally assumed to involve a quark-level Gaussian suppression $\propto \exp(-\pi m^2_{\perp q'}/k)$. This gives all hadrons the same Gaussian $p_\perp$ spectrum. In the thermal model, however, hadrons from the string breaking are generated from an exponential

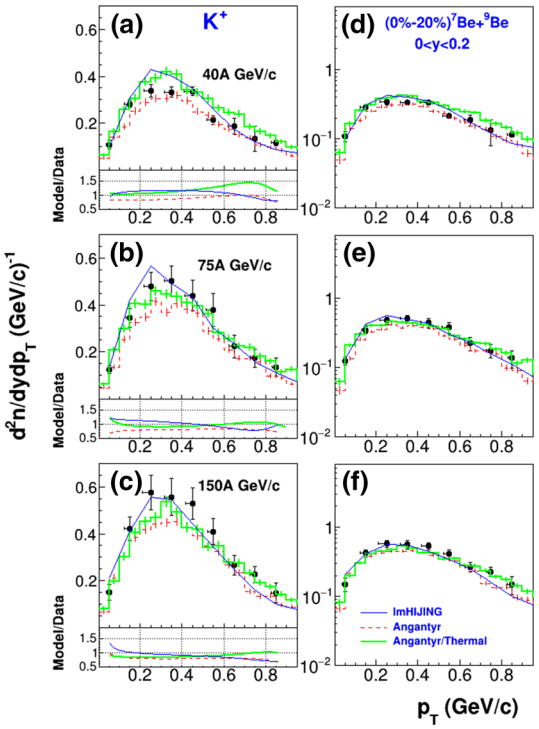

Fig. 11 (COLOR ONLINE) Same as Fig. 10 but for K^+

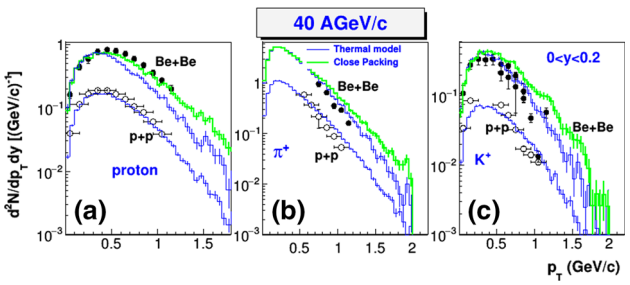

Fig. 12 (COLOR ONLINE) Transverse momentum spectra for protons, π^+ and K^+ in inelastic p+p and 20% central Be+Be collisions. The thermal model calculations with and without close packing of strings are represented by thick and thin lines, respectively. The closed and open points represent NA61/SHINE data [23, 24]

hadron-level suppression like $\exp(-m_{\perp \mathrm{had}}/T)$. Thus, the thermal model, in comparison with the traditional one, enhances low-p_{T} meson production and deplete baryon one. Note that both models determine the longitudinal momentum of the hadron using the Lund string fragmentation function, Eq. 4, with parameters $a = 0.68$ and $b = 0.98$ GeV^{-2}. In Figs. 5, 6, 7, 8, 9, 10, and 11 we explore how the modeling of the two mechanisms impacts the dN/dy and p_{T} spectra of hadrons-pions, kaons, and protons- in central Be+Be collisions at CERN-SPS energies. The thermal model results are represented by thick lines, while the traditional Lund ones by short-dashed lines.

Let us now focus our attention to the stopping of protons. A comparison of the standard Lund and thermal results to the experimental data from the NA61/SHINE collaborations [24] on the rapidity of proton is displayed in Fig. 5. As shown in figure, the discrepancies with respect to the experimental data on the dN/dy can be attributed to a large extend to the different mechanisms of string break-up during hadronization. In particular, the standard Lund model tends to have much stronger stopping as the collision energy decreases, the proton dN/dy distributions are rather flat at $y \sim 0$, while the thermal model shows minima at midrapidity and a rise at projectile/target rapidity in line with the experimental data.

It should be noted that the proton rapidity spectra of other hadron-based models such as UrQMD [19] and AMPT [42] show similar results of large stopping in central Be+Be collisions (see Fig. 31 of Ref. [24]). On the other hand, the hadronic transport model SMASH [22], which employs a distinct Lund symmetric fragmentation function for leading baryons from soft nondiffractive string processes, reproduces the measured proton dN/dy at 40 and 150 AGeV/c. In particular, it is demonstrated in Ref. [22] that harder Lund fragmentation function is preferred by proton, while softer fragmentation functions are applied for all other string fragments. This indicates that particle masses should enter explicitly in the Lund framework for a proper description of identified hadron spectra in central light-ion collisions.

To check the detailed examination of string tunneling mechanisms used in PYTHIA8/Angantyr/HOS model, we show in Fig. 6 the proton p_{T} spectra in midrapidity ($0 < y < 0.2$) central Be+Be collisions. Comparing to the experimental data shows that the traditional Lund model creates more very low-p_{T} protons in the range of $0.1 < p_{\mathrm{T}} < 0.7$ GeV/c for all studied SPS energies. A

drastic improvement of the agreement for the whole SPS energies is obtained with the thermal model calculations. This reflects the expected change that is observed in Fig. 5, where the thermal model leads to more suppression of heavier protons at low p_T. It should be noted that the thermal model is inadequate in describing the high p_T spectra ($p_T > 0.5$) at $p_{beam} > 30$ GeV/c. For 40 AGeV/c, too little p_T is produced for protons, indicating medium effects.

In Figs. 7, 8, and 9 we compare the PYTHIA8/Angantyr/HOS calculations with default Lund and thermal models for the charged pion (the lightest hadron) and charged kaon (strange meson) rapidity spectra at the whole SPS energies in comparison with the data from the NA61/SHINE collaboration [24]. Contrary to the proton dN/dy spectra, the thermal model creates more produced pions and kaons at midrapidity, in accordance with the experimental data. This is due to the fact that the $\exp(-m_{\perp had}/T)$ weight in the thermal model gives more suppression of heavier primary hadron at low-p_T than lighter ones. Therefore, the thermal model provides the best compromise to generate low enough protons, while still producing the right amount of pions and kaons.

Another observation from Fig 7 -in comparison with Fig. 5 is that the default Lund model results systematically overestimate the measured p dN/dy, while the charged pions (negative pions are not shown here) are underestimated. This implies that protons obtain too little longitudinal momentum in the default Angantyr/PYTHIA8 which affects the momentum fraction of the exchanged valence quarks. This results in reducing the string mass, and therefore the energy available for producing new particles is not enough.

Figures 10 and 11 show the transverse momentum distributions of π^+ and K^+ mesons produced at midrapidity ($0 < y < 0.2$) in 20% most central ^{7}Be+ ^{9}Be collisions at 40, 75, and 150 AGeV/c. The Angantyr/HOS/Lund and thermal models are compared to the data at the same meson rapidity. As one can see, the thermal model provides a better description of the π^+ and K^+ p_T-spectra, compared to the default Lund, toward having more multiplicities at both low and high p_T regions. This is due to having an increased mean π^+ and K^+ multiplicities.

Finally, the impact of change of temperature, depending on the close packing of strings (CPS), as in Eq. 7, on the identified hadron spectra is studied in Fig. 12. Here the thermal model results are shown for two cases: including the CPS (thick lines) and without CPS (thin lines) along with the measured proton, π^+ and K^+ p_T spectra at midrapidity in the 20% central Be+Be collisions at 40 AGeV/c. For a clearer picture of the influence of CPS, the results of inelastic p+p collisions are also shown for reference. In p+p collisions, the p_T spectra from the thermal model are in overall good agreement with the measured identified hadron spectra. For central Be+Be collisions, we find that the thermal model calculations of proton p_T spectra, that obtained by Angantyr from interpolation of p+p collisions, show marked deviation and are clearly suppressed at $p_T > 0.5$ GeV/c due to medium effects. We also notice that the thermal model with CPS tends to increase p_T for all particles, which means an improvement for all heavier hadrons, especially protons whose p_T spectrum follows the data remarkably well above 0.5 GeV/c. However, the CPS dependence somewhat increases the π^+, K^+ p_T spectra above 0.5 GeV/c. This indicates that including CPS in the thermal model leads to potentially higher temperatures for central events at midrapidity, where heavy hadrons have a higher probability to be produced at large p_T values, compared to the lighter ones.

It should be noted that other models have also been used to study p_T spectra at midrapidity and rapidity spectra of $\pi^\pm$, $K^\pm$ and protons in the 20% most central ^{7}Be+^{9}Be collisions at SPS energies. The UrQMD (version 3.4) model [19] (which generate hadron cascade based on elementary cross sections for resonance production which either decay (at low energies) or converted into strings which fragment into hadrons (at high energies) accompanied by final hadron scattering) has been compared to the NA61/SHINE data. It is demonstrated in reference [24] that the UrQMD reproduces the p_T spectra of π^- and $K^\pm$ in the 20% most central ^{7}Be+^{9}Be collisions at different SPS energies. In the case of protons and π^- UrQMD, however, overestimates the measurements. On the other hand, the EPOS calculations [43], which includes collective expansion of a thermalized medium, the two-off remnants and elementary scattering represented by a parton ladder, reproduce rather well the measured proton dN/dy and p_T spectra of identified hadrons, while they overestimate the $\pi^\pm$ and $K^\pm$ rapidity spectra at the top SPS energy. The AMPT (version 1.26) [42], the PHSD (version 4.0) [21] also fail in describing the rapidity distribution of the NA61/SHINE data.

4 Summary and conclusions

In order to investigate the differences among string-based models on hadron spectra, we compare the updated HIJING and PYTHIA8/Angantyr models with the recent NA61/SHINE data of proton, $\pi^\pm$ and $K^\pm$ rapidity and transverse momentum spectra in the 20% most central ^{7}Be+^{9}Be collisions at CERN SPS energies. In the present work, the HIJING (version 1.383) code is extended with a more modern version of PYTHIA (version 6.4), which includes both the hard QCD and the standard Lund string routines of PYTHIA8. As for Angantyr, the initial conditions for light nuclei ($A \leq 16$) are updated with a GLISSANDO (Glauber initial state simulation and more) harmonic oscillator shell (HOS) model density profile. The main source of difference between Angantyr and HIJING at intermediate energies ($\sqrt{s_{NN}} \leq 20$ GeV) is the different treatment of generation of diffractive-like events: While Angantyr generates low/high-mass diffraction events using Pomeron flux, HIJING treats the (non)diffractively excited nucleons as in FRITIOF model. Such diffractive-like events lead to longitudinal string-like excitations which then hadronized according to the Lund string fragmentation scheme. It is shown that neither of the models provides a satisfactory description of the measured hadron spectra at CERN SPS energies completely.

We have also investigated the effects of other string fragmentation models implemented in PYTHIA8, namely, the Schwinger-model like and the thermal ones, on hadron production. The thermal model is intended to enhance low $p_\perp$ light-hadron production,

relative to the heavier ones. In contrast, all hadrons receive the same $p_\perp$ spectrum for the traditional Schwinger-model. We find that the thermal model contributes to some aspects of the inclusive spectra in central Be+Be collisions; notably, the reduction of low $p_\perp$ protons and enhancement of pions(kaons) yields at midrapidity. This helps to remedy the glaring discrepancy of proton stopping of the traditional PYTHIA8 event generator in comparisons with NA61/SHINE data.

Thus, the main features of PYTHIA8/Angantyr/HOS, with the thermal model, are the ability to reproduce proton, $\pi^\pm$ and $K^\pm$ in central light-ion beams at CERN SPS energies. This may imply that the model may be considered as one of the possible candidates of Monte Carlo event generators to study heavy-ion collisions at CERN-SPS energies.

Acknowledgements The authors would like to thank the Deanship of Scientific Research at Umm Al-Qura University for supporting this work by Grant Code: (22UQU4331268DSR03).

Data availibility This manuscript has no associated data or the data will not be deposited. Author's comment: Presented calculations can be easily reproduced. Thus there is no need to deposit them as data.

References

1. X.-N. Wang, M. Gyulassy, Phys. Rev. D **44**, 3501 (1991)
2. W.-T. Deng, X.-N. Wang, R. Xu, Phys. Rev. C **83**, 014915 (2011)
3. W.-T. Deng, X.-N. Wang, R. Xu, Phys. Lett. B **701**, 133 (2011)
4. T. Sjöstrand et al., Comp. Phys. Comm. **191**, 159–177 (2015)
5. Christian Bierlich, Gösta. Gustafson, Leif Lönnblad, Harsh Shah, JHEP **10**, 134 (2018)
6. P. Skands, S. Carrazza, J. Rojo, Eur. Phys. J. C **74**, 3024 (2014)
7. A.M. Sirunyan et al., Eur. Phys. J. C **80**, 4 (2020)
8. M.S. Abdallah et al., STAR Collaboration. Phys. Rev. D **103**, L091103 (2021)
9. J. Adam et al., STAR Collaboration. Phys. Rev. D **101**, 05200052004 (2020)
10. B. Andersson, G. Gustafson, G. Ingelman, T. Sjöstrand, Phys. Rep. **97**, 31–145 (1987)
11. G.A. Schuler, T. Sjöstrand, Phys. Rev. D **49**, 2257 (1994)
12. B. Andersson, G. Gustafson, B. Nilsson-Almqvist, Nucl. Phys. B **281**, 289 (1987)
13. B. Nilsson-Almqvist, E. Stenlund, Comp. Phys. Comm. **43**, 387 (1987)
14. Torbjörn Sjöstrand, Comput. Phys. Commun. **82**, 74 (1994)
15. J. Schwinger, Phys. Rev. **83**, 664 (1951)
16. B. Andersson, G. Gustafson, B. Söderberg, Z. Phys. C **20**, 317 (1983)
17. T. Sjöstrand, S. Mrenna, P. Skands, J. High Energy Phys. **2006**, 026 (2006)
18. P.Z. Skands, Phys. Rev. D **82**, 074018 (2010)
19. S. Bass et al., Prog. Part. Nucl. Phys. **41**, 255 (1998)
20. O. Bus et al., Phys. Rep. **512**, 1 (2012)
21. W. Cassing, E.L. Bratkovskaya, Phys. Rev. C **78**, 034919 (2008)
22. J. Weil et al., Phys. Rev. C **94**, 054905 (2016)
23. A. Aduszkiewicz et al., NA61/SHINE collaboration. Eur. Phys. J. C **77**, 671 (2017)
24. A. Acharya, NA61/SHINE collaboration. Eur. Phys. J. C **81**, 73 (2021)
25. V. Kireyeu, I. Grishmanovskii, V. Kolesnikov, V. Voronyuk, E. Bratkovskaya, Eur. Phys. J. A **56**, 223 (2020)
26. Wojciech Broniowski, Maciej Rybczyński, Piotr Bożek, Comp. Phys. Comm. **180**, 69 (2009)
27. Khaled Abdel-Waged, Nuha Felemban, J. Phys. G **47**, 065104 (2020)
28. R.V. Poberezhnyuk, M. Gazdzicki, M.I. Gorenstein, Acta Phys. Polon. B **46**, 1991 (2015)
29. A. Motornenko, V.V. Begun, V. Vovchenko, M.I. Gorenstein, H. Stoecker, Phys. Rev. C **99**(3), 034909 (2019)
30. Nadine Fischer, Torbjörn Sjöstrand, J. High Energy Phys. **2017**, 140 (2017)
31. Khaled Abdel-Waged, Eur. Phys. J. C **82**, 65 (2022)
32. A. Acharya, NA61/SHINE collaboration. Eur. Phys. J. C **80**, 961 (2020)
33. A. Acharya, NA61/SHINE collaboration. Eur. Phys. J. C **81**, 397 (2021)
34. H.J. Drescher et al., Phys. Rept. **350**, 93 (2001)
35. A. Bialas, M. Bleszynski, W. Czyz, Nucl. Phys. B **111**, 461 (1976)
36. R. Hagedorn, Multiplicities. Riv. Nuovo Cim. **6**(10), 1 (1983)
37. S. Barshay, Y.A. Chao, Phys. Lett. B **38**, 225 (1972)
38. C. Tsallis, J. Statist. Phys. **52**, 479 (1988)
39. A.A. Bylinkin, A.A. Rostovtsev, Phys. Atom. Nucl. **75**, 999 (2012)
40. Khaled Abdel-Waged, Nuha Felemban, Phys. Rev. C **105**, 024909 (2022)
41. A. Donnachie, P.V. Landshoff, Phys. Lett. B **296**(227), 232 (1992)
42. Z.W. Lin, C.M. Ko, Phys. Rev. C **65**, 034904 (2002)
43. K. Werner, Nucl. Phys. B - Proc. Suppl. **175–176**, 81–87 (2008)